Supporting Information

Chlorination *vs*. fluorination: a study of halogenated benzo[c][1,2,5]thiadiazole-based organic semiconducting dots for near-infrared cellular imaging

Daize Mo,[ab] Li Lin, [c] Pengjie Chao,[b] Hanjian Lai,[b] Qingwen Zhang,[*a] Leilei Tian [*c] and Feng He[*b]

a. State Key Laboratory of Quality Research in Chinese Medicine and Institute of Chinese Medical Sciences, University of Macau, 999078, Macao, P. R. China. E-mail: qwzhang@um.edu.mo

b. Department of Chemistry and Guangdong Provincial Key Laboratory of Catalysis, Southern University of Science and Technology, Shenzhen, 518055, China. E-mail: hef@sustech.edu.cn

c. Department of Materials Science and Engineering, South University of Science and Technology, Shenzhen, 518055, P. R. China. E-mail: tianll@sustech.edu.cn

1. General Methods

1.1 Chemicals and reagents

3-Dodecylthiophene, tri-*n*-butyltinchloride ((*n*-Bu)$_3$SnCl), *n*-butyllithium (*n*-BuLi), 4-(diphenylamino)phenylboronicacid, 4-fluro-1,2-diaminobenzene, 4,5-difluoro-1,2-benzenediamine, 4-chloro-5-fluoro-1,2-diaminobenzene, 4-chloro-1,2-diaminobenzene, 4,5-dichloro-1,2-benzenediamine, thionyl chloride ($SOCl_2$), pyridine, hydrobromic acid (HBr), bromine (Br_2), tetra-kis(triphenylphosphine)palladium(0) ($Pd(PPh_3)_4$, and *N*-bromosccinimide (NBS) were purchased from commercial sources and used directly. Sodium Carbonate (Na_2CO_3) was purchased from Damao Chemical Reagent Company (Tianjin, China). Poly (styrene-maleic anhydride) (PSMA, average Mw = 1700, styrene content approximately 68%) was purchased from Sigma-Aldrich. Before the reaction, tetrahydrofuran (THF) and toluene were distilled from the sodium/benzophenone under the protection of nitrogen atmosphere. Human alveolar epithelial cells (A549) were kindly provided by Professor Ying Sun at the Department of Biology of Southern University of Science and Technology (SUSTech).

1.2 Measurements

^{1}H NMR spectra was determined by Bruker Avance-400 (400 MHz) spectrometers. Thermogravimetric analysis (TGA) plots were conducted on a Discovery series instrument under a nitrogen atmosphere with a heating rate of 10 °C /min in N_2. Cyclic voltammetry was performed on a Model CHI 660E potentiostat/galvanostat (Shanghai Chenhua Instrumental Co., Ltd. China) to determine the HOMO and LUMO levels of the monomers, in an dichloromethane solution of 0.1 mol L^{-1} tetrabutylammonium hexafluorophosphate (*n*-Bu_4NPF_6) at a potential scan rate of 100 mV s^{-1} with an Ag/Ag+ reference electrode and a platinum wire counter electrode under an argon atmosphere. The redox potential of ferrocene/ferrocene$^+$ (Fc/Fc^+) under the same conditions is located at 0.044 V, which is assumed to have an absolute energy level of -4.8 eV to vacuum. The UV-visible absorption spectrum of **FBT-DiTPA, FFBT-DiTPA, FClBT-DiTPA, ClBT-**

DiTPA, and **ClClBT-DiTPA** molecules and its corresponding dots was carried out by Shimadzu UV-3600 PC in the range of 300-800 nm. The steady-state fluorescence spectrum was carried out on Shimadzu RF5301 PC fluorescence spectrometer. The photo-stability the fluorinated/chlorinated dots were carried out under the xenon lamp which equipped with a xenon lamp. The dots size was determined by NanoBrook Omni dynamic light scattering and Hitachi H-600 transmission electron microscope. The cytotoxicity of the dots was determined by a Cytation 3 microplate reader, and the fluorescence imaging of the cells was performed by a Leica TCS-SP8 laser scanning confocal microscope.

1.3. Preparation of dots

The **FBT-DiTPA**, **FFBT-DiTPA**, **FClBT-DiTPA**, **ClBT-DiTPA**, and **ClClBT-DiTPA** dots were all prepared by the nano-reprecipitation method. At first, the chlorinated/fluorinatied molecules and PSMA were dissolved in THF with the final concentration solution was 1 mg/mL, respectively. Next, 500 μL chlorinated/fluorinatied molecules solution and 100 μL PSMA solution were diluted with 9400 μL anhydrous THF to get the mixed solution. Under intense ultrasound, 5 mL mixture was quickly poured into a 50 ml glass bottle which containing 10 mL water for 10 minutes. After that, the THF was removed on a rotary evaporator at 50 °C completely. After cooling to room temperature, the dots solution was filtered through a 0.22 micron filter to remove the fraction of aggregates. As prepared dots was very stable without the phenomenon of aggregation after several months of storage.

1.4. MTT Assay

The MTT method was conducted to test the toxicity of **FBT-DiTPA**, **FFBT-DiTPA**, **FClBT-DiTPA**, **ClBT-DiTPA**, and **ClClBT-DiTPA** dots. The A549 cell suspension and an equal volume of PBS were added to a 96-well plate (5000

cells/well), and incubated at 37 °C overnight. Then the fresh cell culture media containing a series of concentrations of 0, 5, 10, 20, and 40μg/mL of the **FBT-DiTPA**, **FFBT-DiTPA**, **FClBT-DiTPA**, **ClBT-DiTPA**, and **ClClBT-DiTPA** dots were added and incubated for 24 h, respectively. After that, we then washed the cells 3 times with PBS to remove the free chlorinated/fluorinatied dots. After shaking 10 minutes at 25°C, the absorbance at 490 nm was determined to calculate the survival rate of the cells.

1.5. Cell imaging

Ten thousand cultured A549 cells were digested and plated on a six-well plate, adherent to the glass wall overnight. After removing the medium, it was washed with PBS repeat. 1.5 mL 40 g/mL solution of the five dots was added, incubated at 37°C for 4 hours, and the PBS (pH 7.4) buffer was used to remove the excess dots. At last, the confocal images of the cells were performed by a Leica SPE laser scanning confocal microscope. All the dots were excited at 632 nm and the fluorescence of them was collected at 650-700 nm.

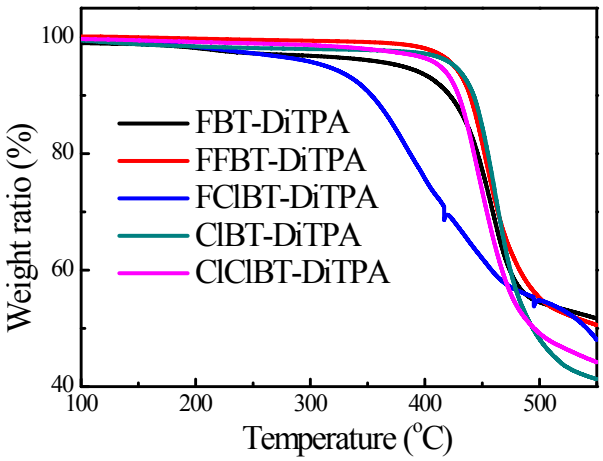

Figure S1. The thermogravimetry of the chlorinated / fluorinated materials.

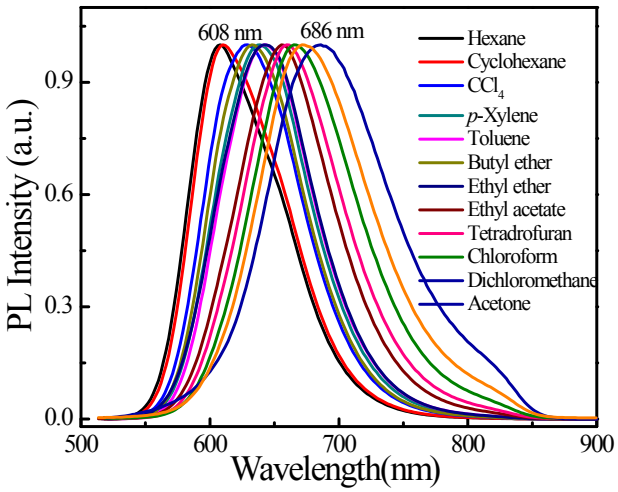

Figure S2. PL spectra of **FBT-DiTPA** in different solvents.

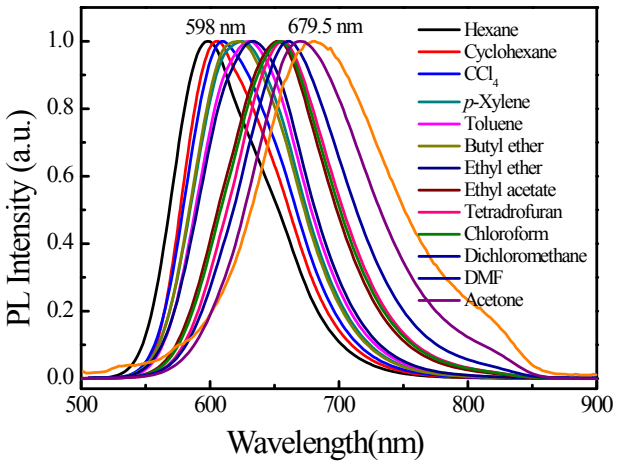

Figure S3. PL spectra of **FFBT-DiTPA** in different solvents.

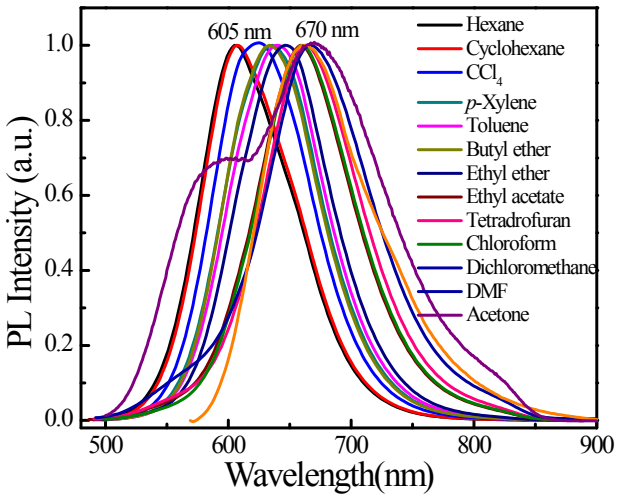

Figure S4. PL spectra of **FClBT-DiTPA** in different solvents.

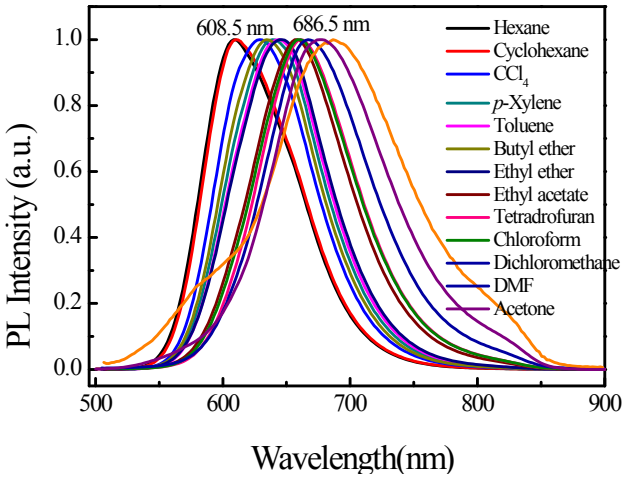

Figure S5. PL spectra of **ClBT-DiTPA** in different solvents.

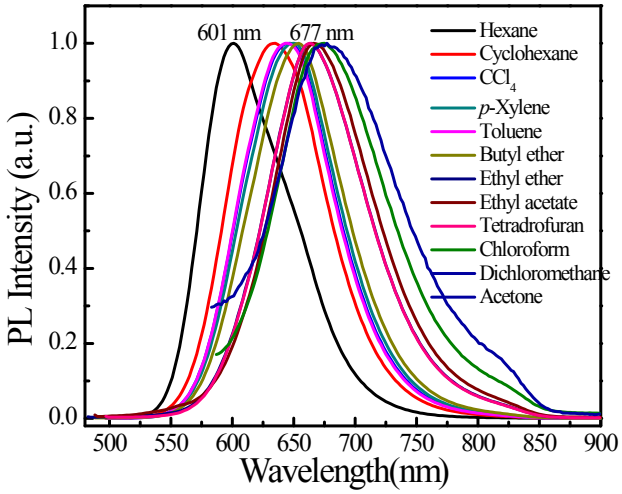

Figure S6. PL spectra of **ClClBT-DiTPA** in different solvents.

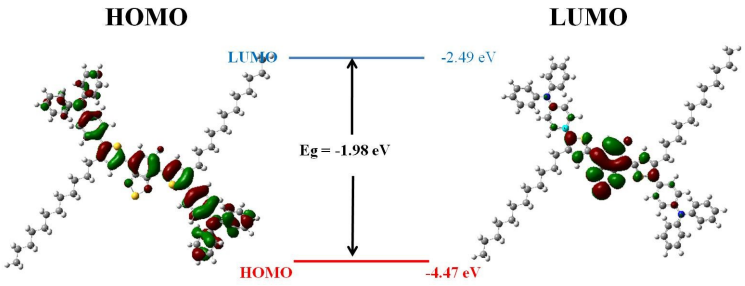

Figure S7. B3LYP/6-31G calculated HOMO and LUMO density maps of **FBT-DiTPA**.

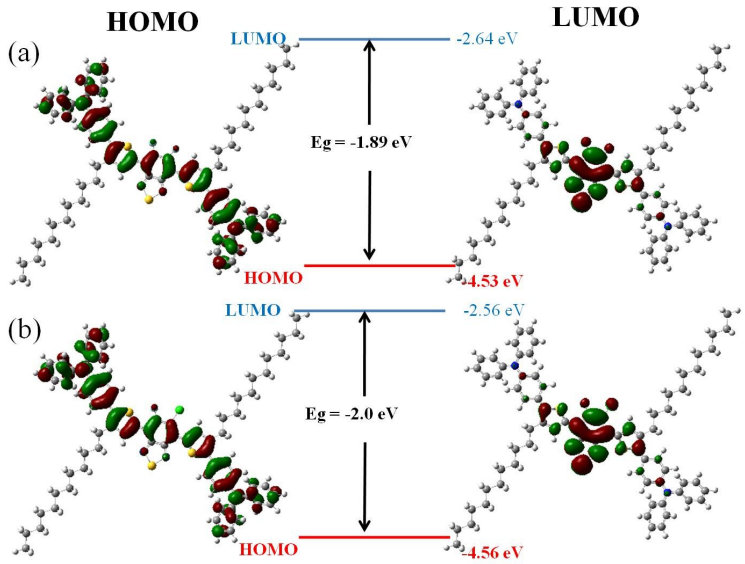

Figure S8. B3LYP/6-31G calculated HOMO and LUMO density maps of **FFBT-DiTPA** and **FClBT-DiTPA**.

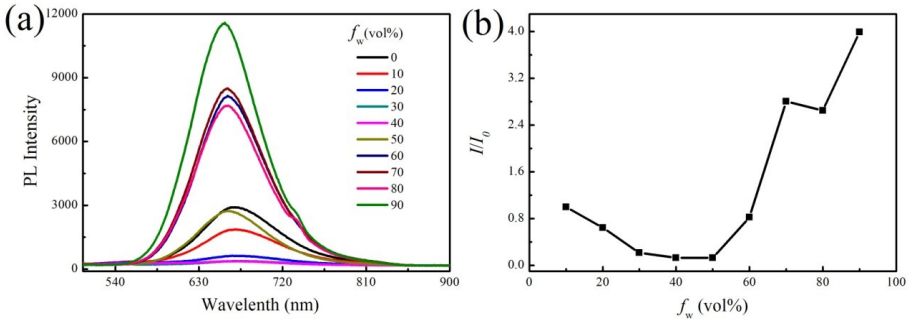

Figure S9. (a) PL spectra of **ClClBT-D-iTPA** in tetrahydrofuran (THF)-water mixtures with different water fractions (f_w). (b) Plots of I/I_0 *vs* water fractions in THF-water mixtures. I_0 is the PL intensity in pure THF.

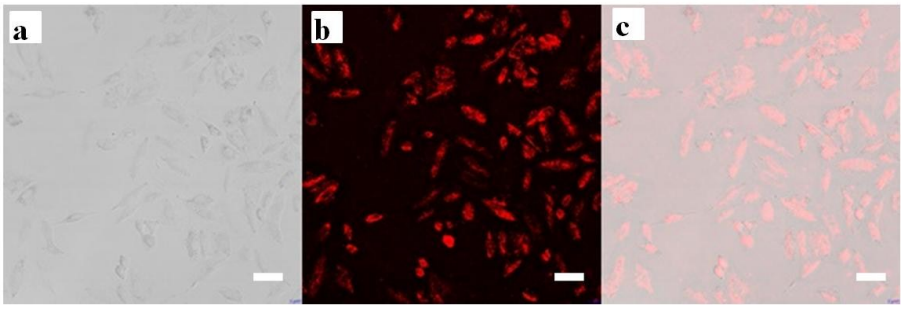

Figure S10. CLSM images ofA549 cells incubated with 40 μg/mL **FBT-DiTPA** dots for 4 h. From left to right are bright field images (A), fluorescence images (B), and combined bright field and fluorescence images (C). Scale bar=25μm.

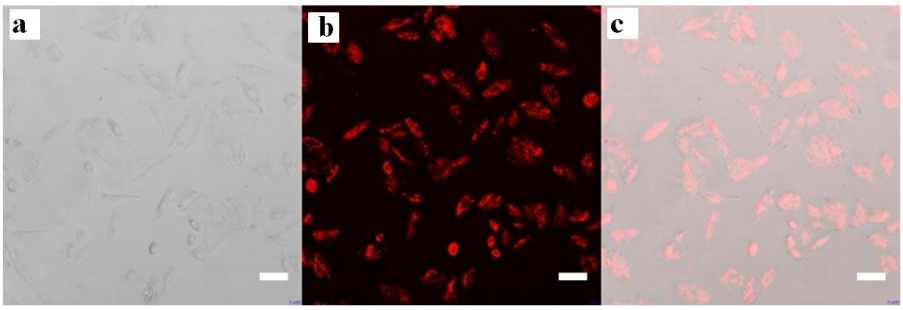

Figure S11. CLSM images of A549 cells incubated with 40 μg/mL **FFBT-DiTPA** dots for 4 h. From left to right are bright field images (A), fluorescence images (B), and combined bright field and fluorescence images (C). Scale bar=25μm.

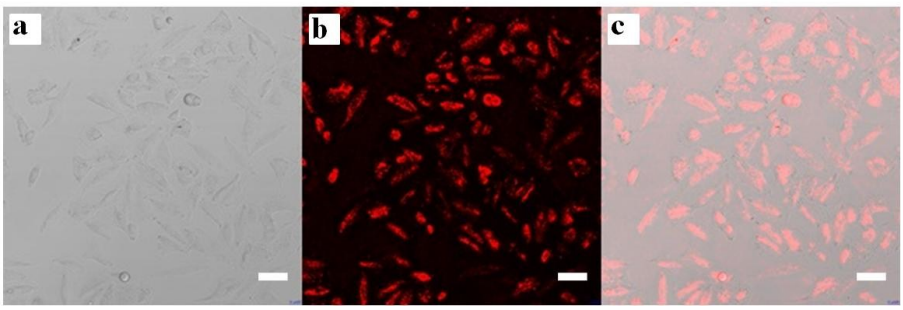

Figure S12. CLSM images of A549 cells incubated with 40 μg/mL **FClBT-DiTPA** dots for 4 h. From left to right are bright field images (A), fluorescence images (B), and combined bright field and fluorescence images (C). Scale bar=25μm.

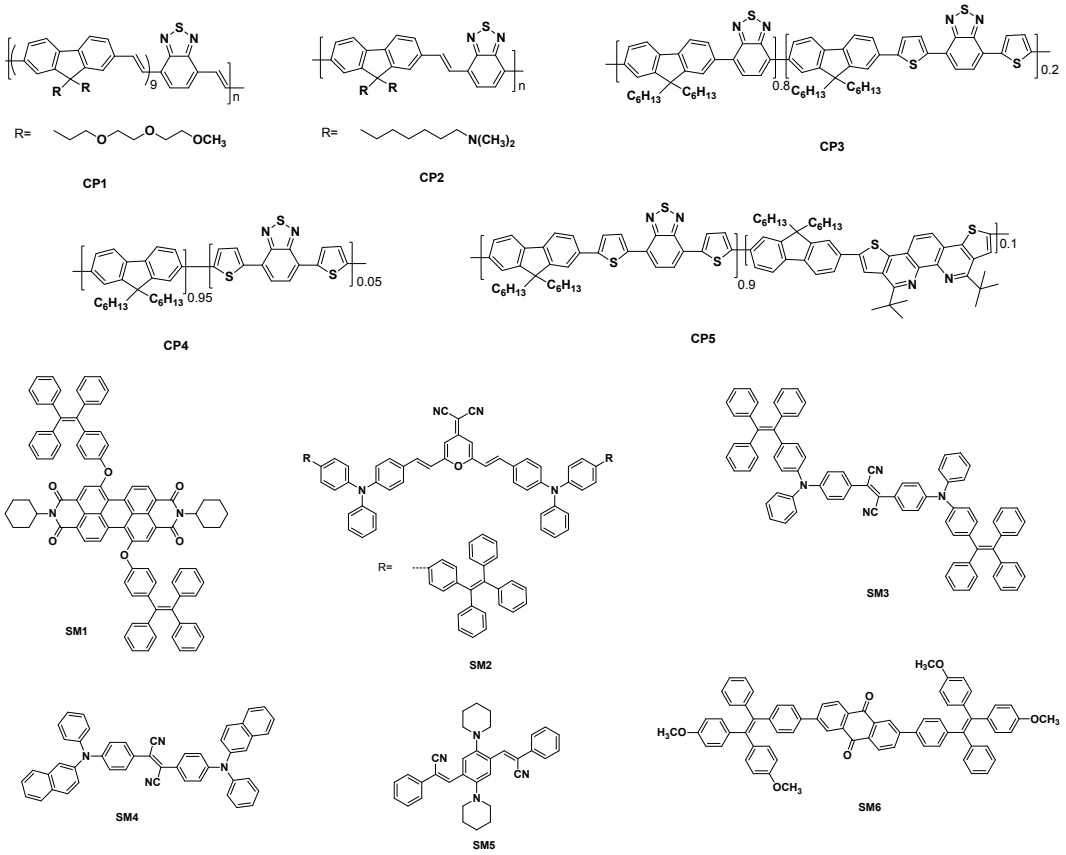

Figure S13. Chemical structures of some previously reported compounds for the fluorescence imaging applications.

Table S1. Summary of previously reported compounds for fluorescence imaging applications.

Compounds	Size (nm)	λ_{ex} (nm)	λ_{em} (nm)	Q_Y (%)	Application
CP1	193	436	622	19	In vitro cell imaging[1]
CP2	180	516	636	7	In vivo dual-modality tumor imaging[2]
CP3	80	550	698	27	In vitro/in vivo targeted cell/tumor imaging[3]
CP4	-	-	650	55	In vivo brain tumor targeting[4]
CP5	13	369, 515	677	6.2	In vitro cell imaging[5]
SM1	57	514	680	8	In vitro targeted cell tracing[6]
SM2	148	505	668	12	In vivo cell imaging[7]
SM3	30	511	671	24	In vitro/in vivo cell tracing[8]
SM4	70	475	650	14.9	In vivo targeted tumor imaging[9]
SM5	25	349	653	20	In vitro cell imaging [10]
SM6	28.2	335	650	3.9	Photodynamic therapy [11]

1. K. Li, R. Zhan, S. Feng and B. Liu. *Anal. Chem*., 2011, **83**, 2125-2132.
2. K. Li, D. Ding, D. Huo, K. Y. Pu, N. N. P. Thao, Y. Hu, Z. Li and B. Liu. *Adv. Funct. Mater*., 2012, **22**, 3107-3115.
3. D. Ding, J. Liu, G. Feng, K. Li, Y. Hu and B. Liu. *Small*, 2013, **9**, 3093-3102.
4. C. Wu, S. J. Hansen, Q. Hou, J. Yu, M. Zeigler, Y. H. Jin, D. R. Burnham, J. D. McNeill, J. M. Olson and D. T. Chiu. *Angew. Chem., Int. Ed*., 2011, **50**, 3430-3434.
5. C. Yan, Z. Sun, H. Guo, C. Wu and Y. Chen. *Mater. Chem. Front*., 2017, **1**, 2638-2642.
6. Q. Zhao, K. Li, S. Chen, A. Qin, D. Ding, S. Zhang, Y. Liu, B. Liu, J. Z. Sun and B. Z. Tang. *J. Mater. Chem*., 2012, **22**, 15128-15135.
7. W. Qin, D. Ding, J. Liu, W. Z. Yuan, Y. Hu, B. Liu and B. Z. Tang. *Adv. Funct. Mater*., 2012, **22**, 771-779.
8. K. Li, W. Qin, D. Ding, N. Tomczak, J. Geng, R. Liu, J. Liu, X. Zhang, H. Liu, B. Liu and B. Z. Tang. *Sci. Rep*., 2013, **3**, 1150.

9. Y. Yang, F. An, Z. Liu, X. Zhang, M. Zhou, W. Li, X. Hao, C. S. Lee and X. Zhang. *Biomaterials*, 2012, **33**, 7803-7809.
10. Y. Zhang, K. Chang, B. Xu, J. Chen, L.Yan, S. Ma, C. Wu and W. Tian. *RSC Adv*., 2015, 5, 36837-36844.
11. G. Feng, W. Wu, S. Xu and B. Liu. *ACS Appl. Mater. Interfaces*, 2016, **8**, 21193-21200.

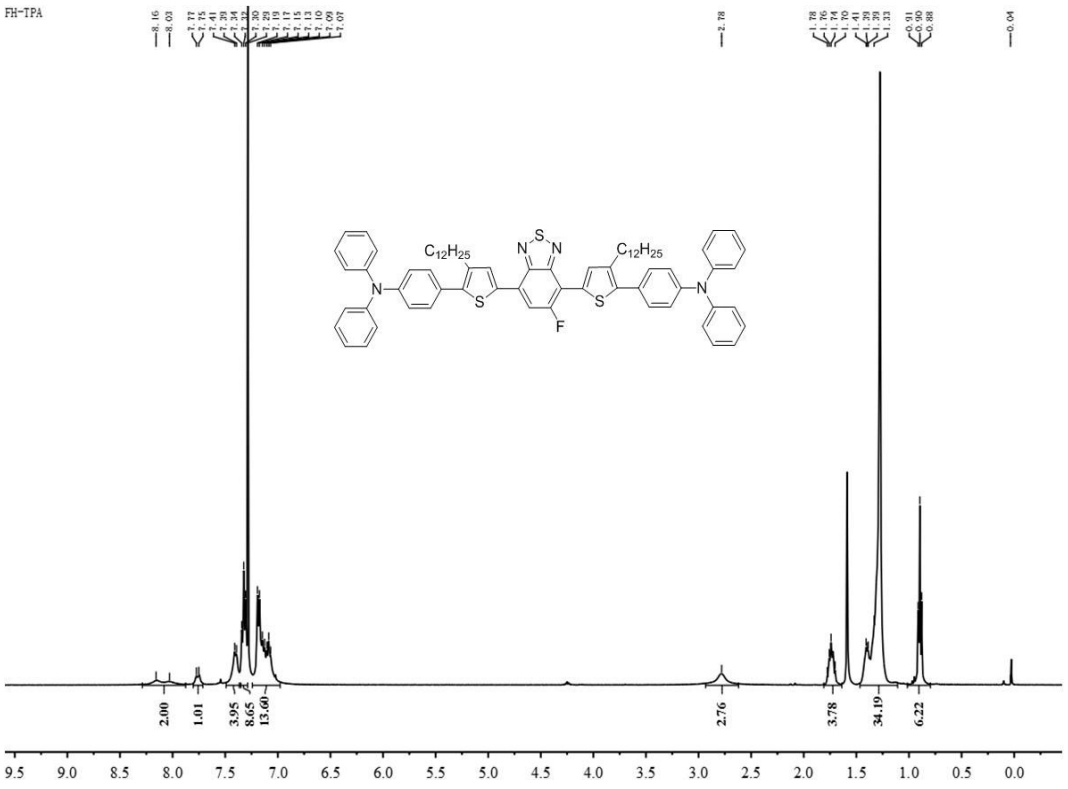

Figure S14. ^{1}H NMR spectrum of **FBT-DiTPA** in $CDCl_3$.

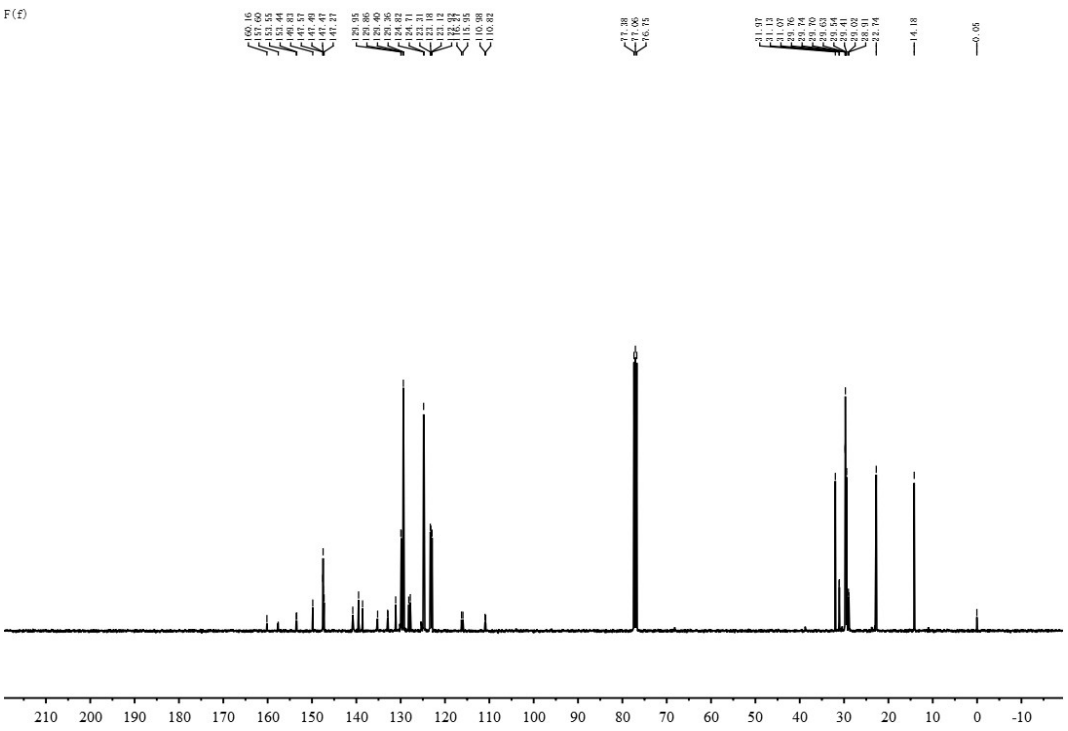

Figure S15. ^{13}C NMR spectrum of **FBT-DiTPA** in $CDCl_3$.

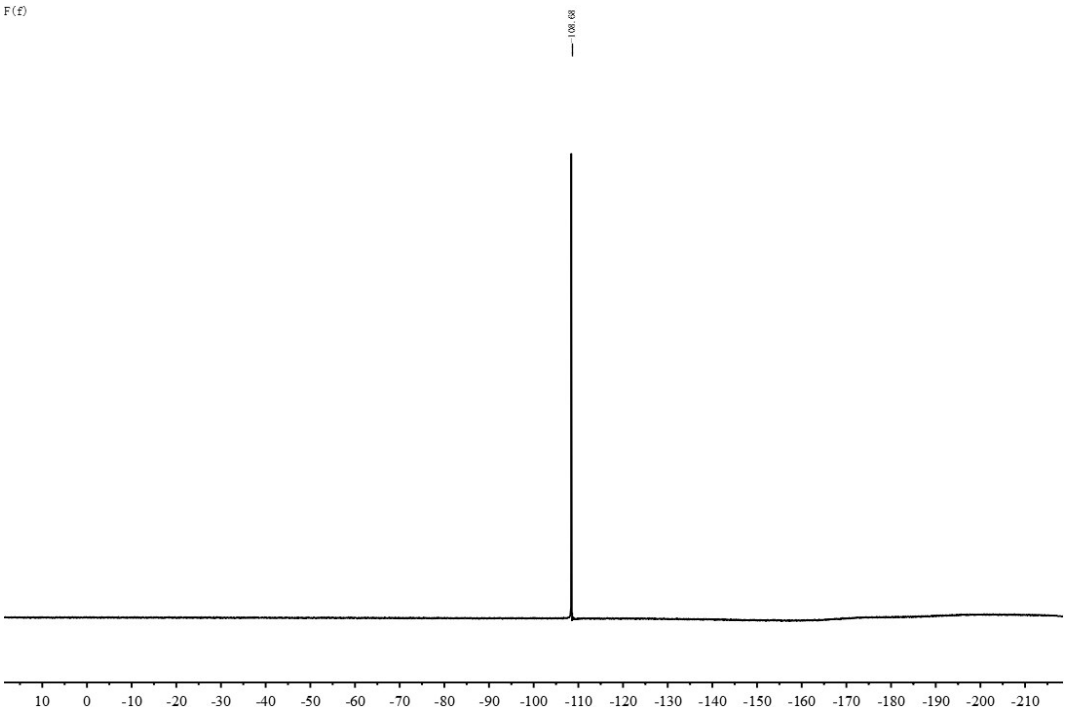

Figure S16. ^{19}F NMR spectrum of **FBT-DiTPA** in $CDCl_3$.

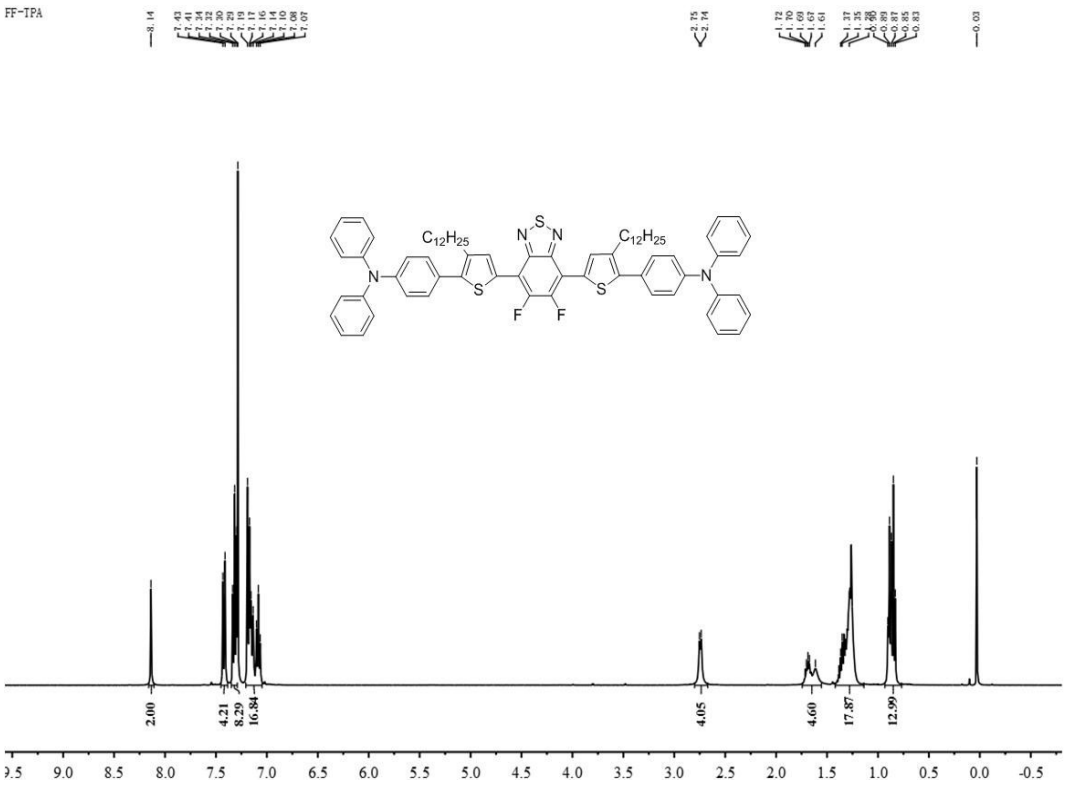

Figure S17. ^{1}H NMR spectrum of **FFBT-DiTPA** in $CDCl_3$.

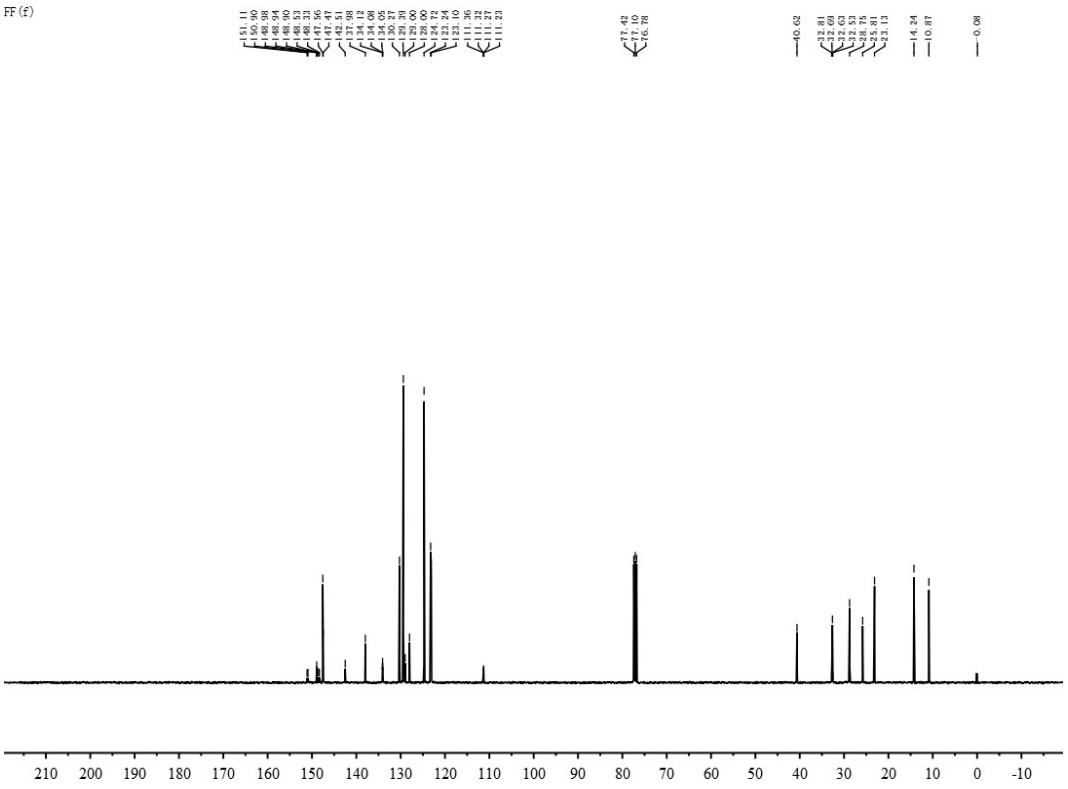

Figure S18. ^{13}C NMR spectrum of **FFBT-DiTPA** in $CDCl_3$.

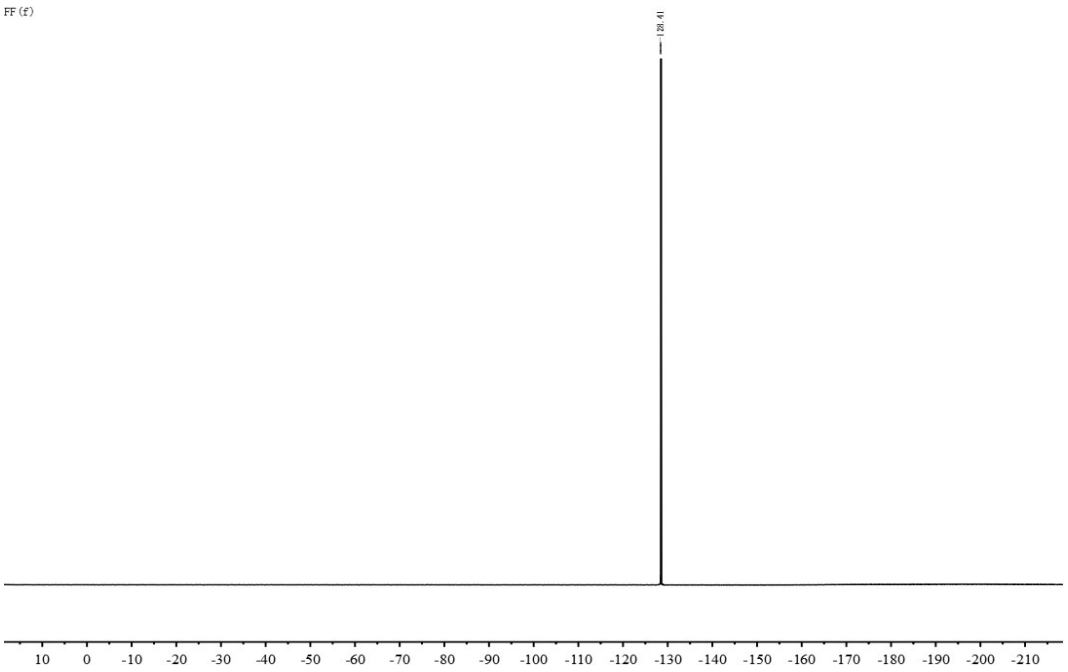

Figure S19. ^{19}F NMR spectrum of **FBT-DiTPA** in $CDCl_3$.

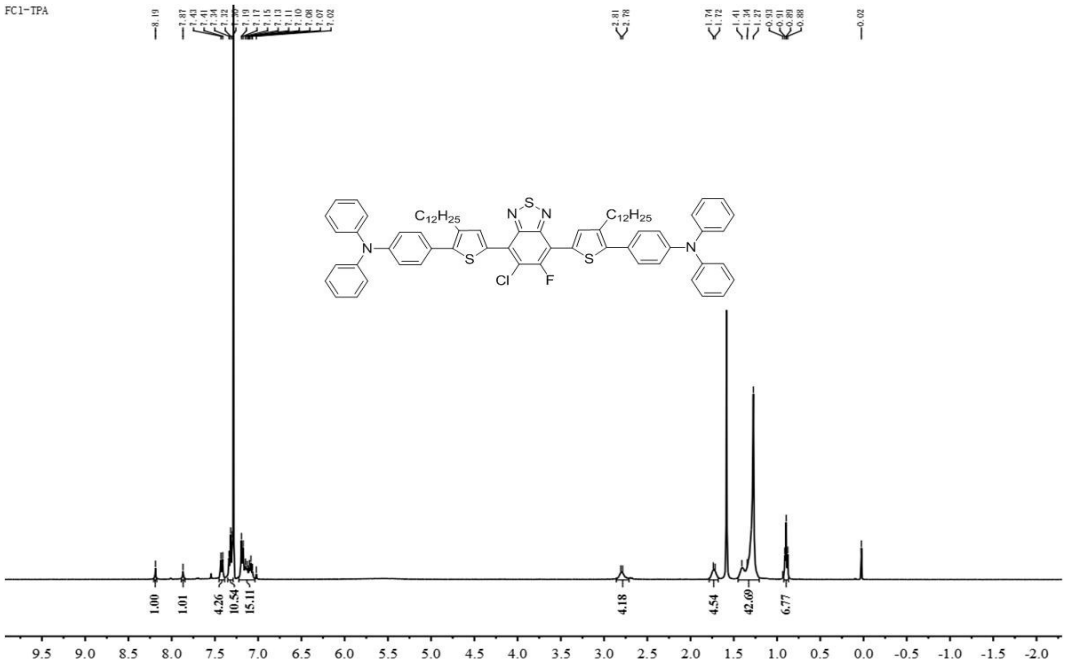

Figure S20. ^{1}H-NMR spectrum of **FClBT-DiTPA** in $CDCl_3$.

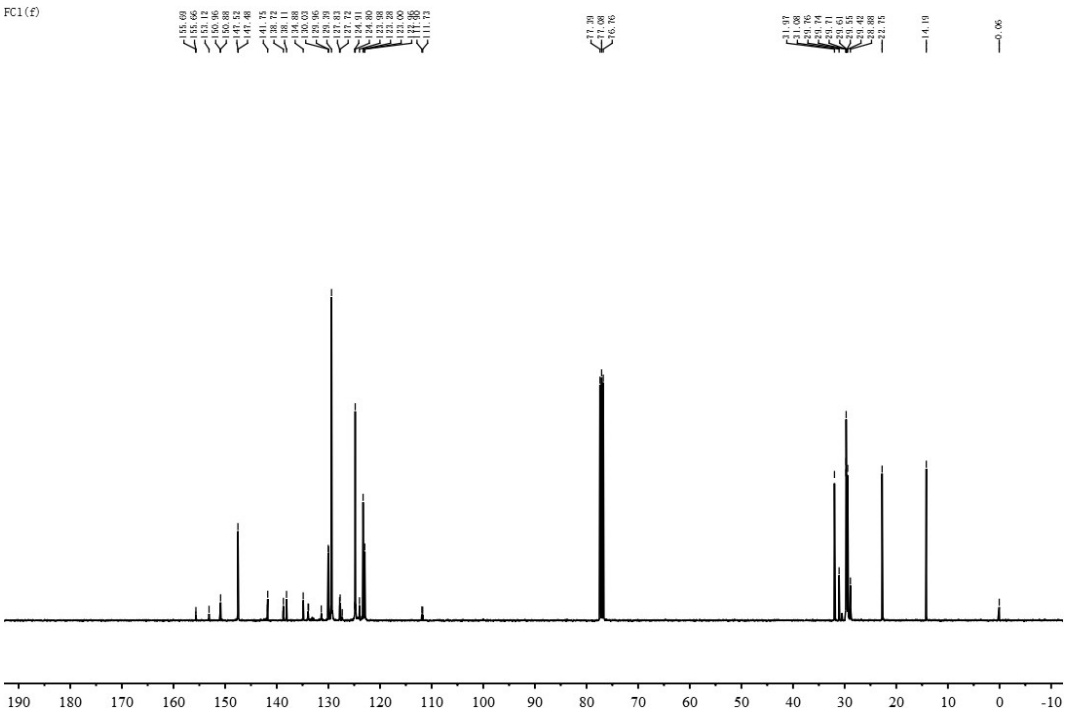

Figure S21. ^{13}C NMR spectrum of **FClBT-DiTPA** in $CDCl_3$.

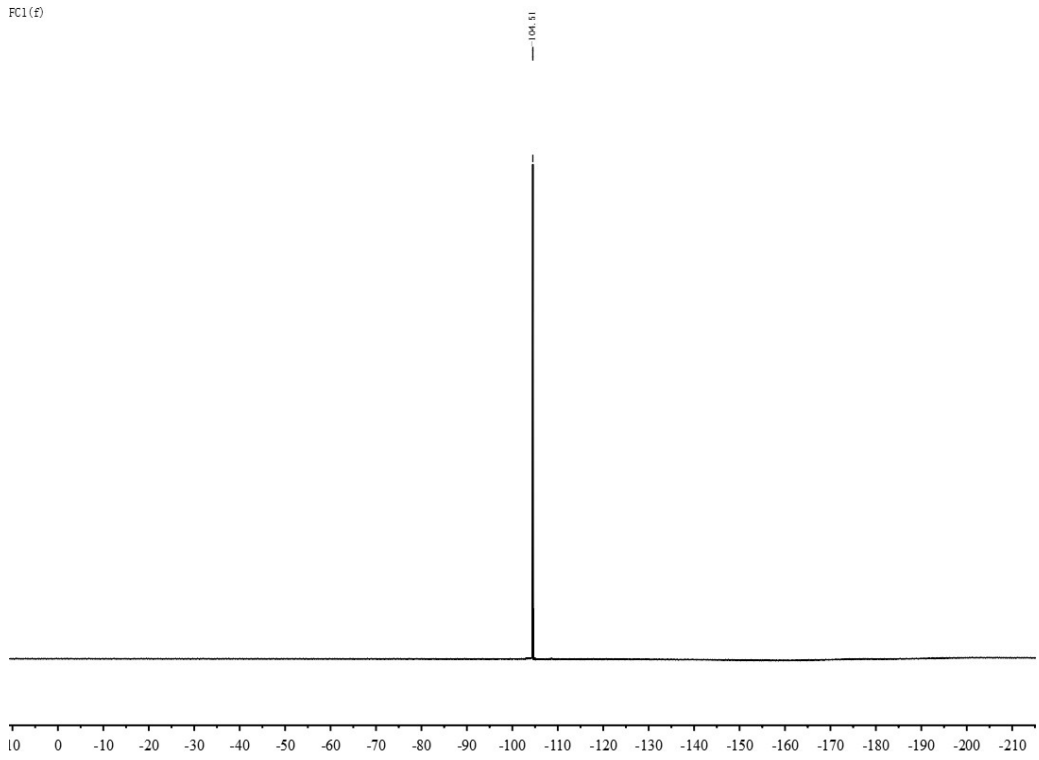

Figure S22. ^{19}FNMR spectrum of **FBT-DiTPA** in $CDCl_3$.

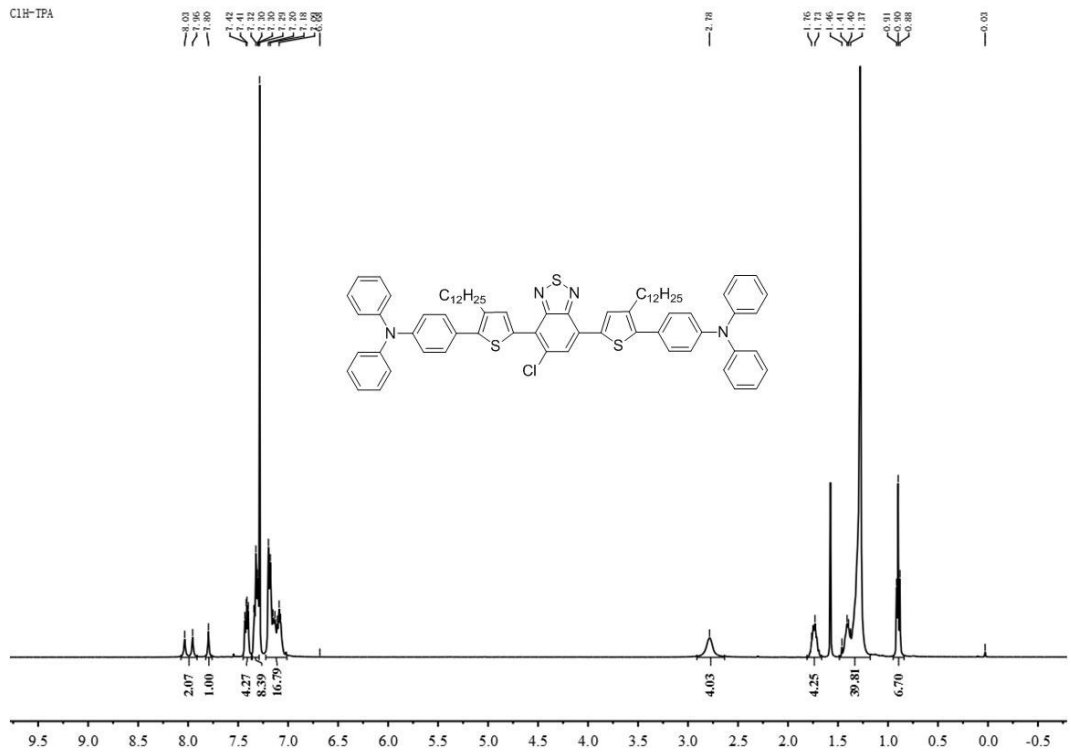

Figure S23. ^{1}H NMR spectrum of **ClBT-DiTPA** in $CDCl_3$.

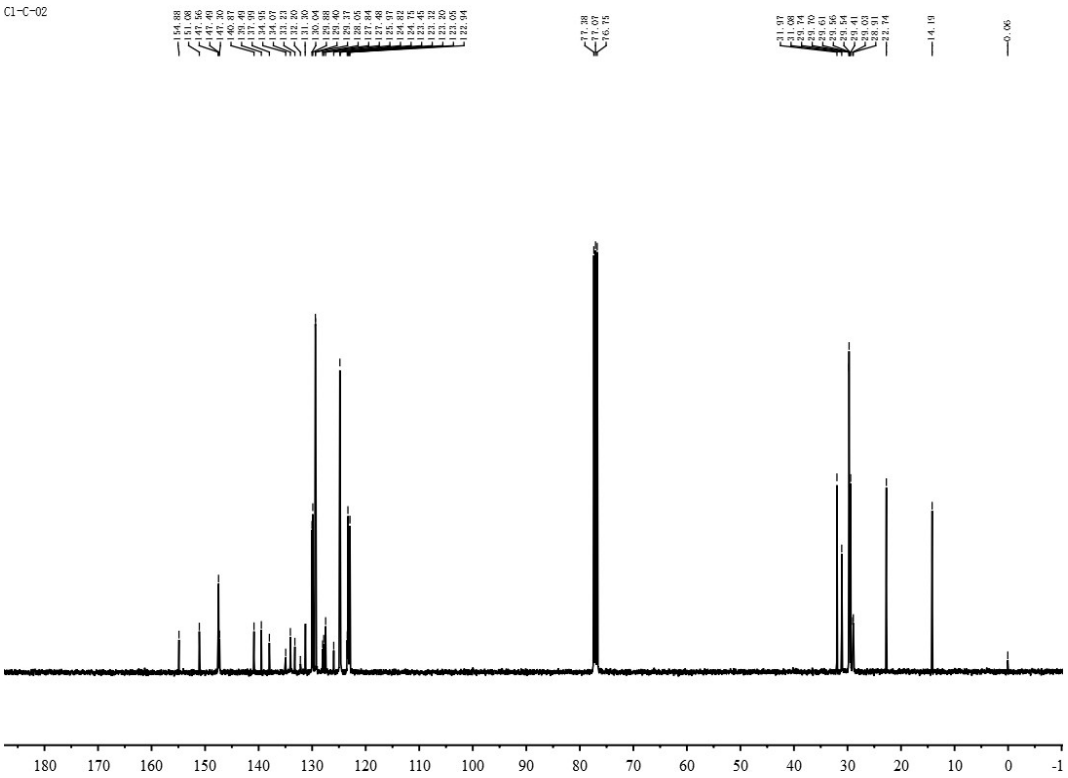

Figure S24. ^{19}C NMR spectrum of **ClBT-DiTPA** in $CDCl_3$.

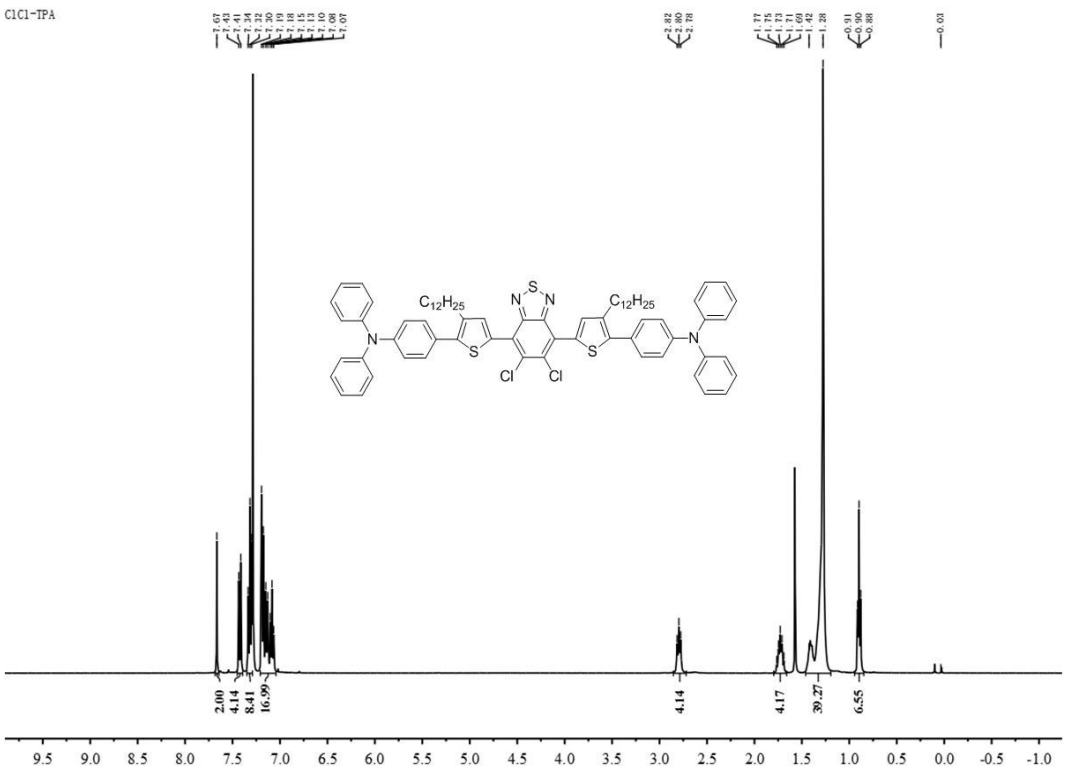

Figure S25. ^{1}H-NMR spectrum of **ClClBT-DiTPA** in $CDCl_3$.

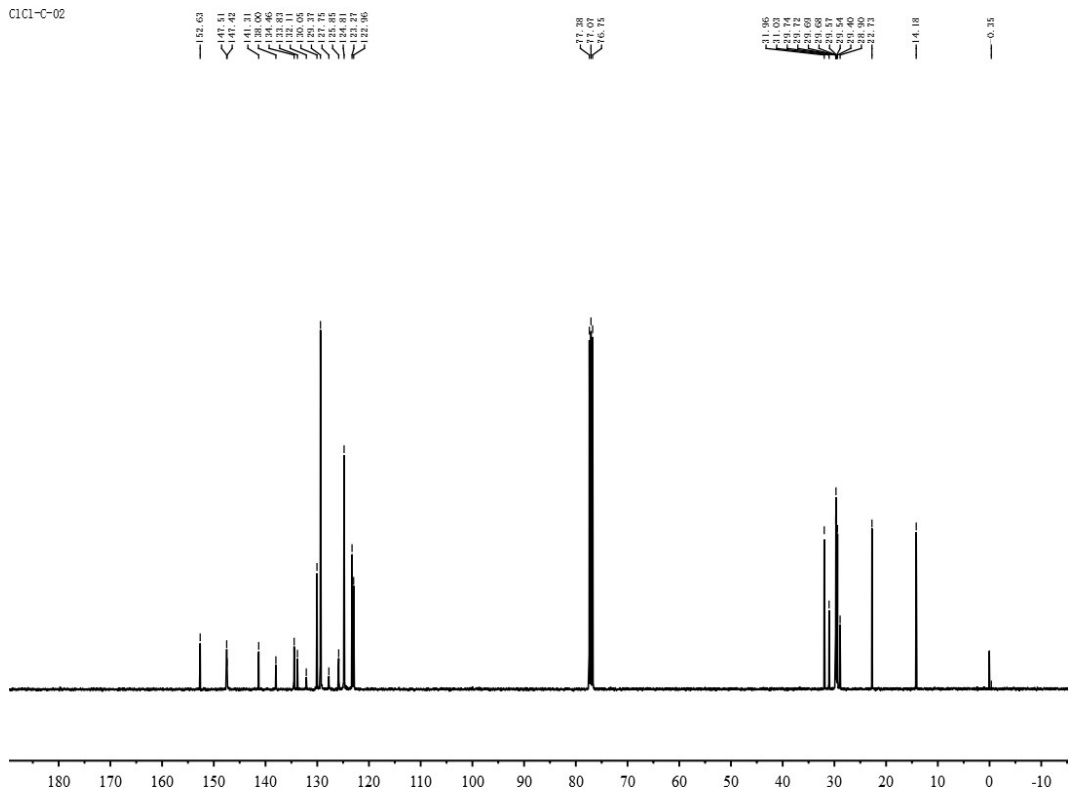

Figure S26. ^{13}C NMR spectrum of **ClClBT-DiTPA** in $CDCl_3$.

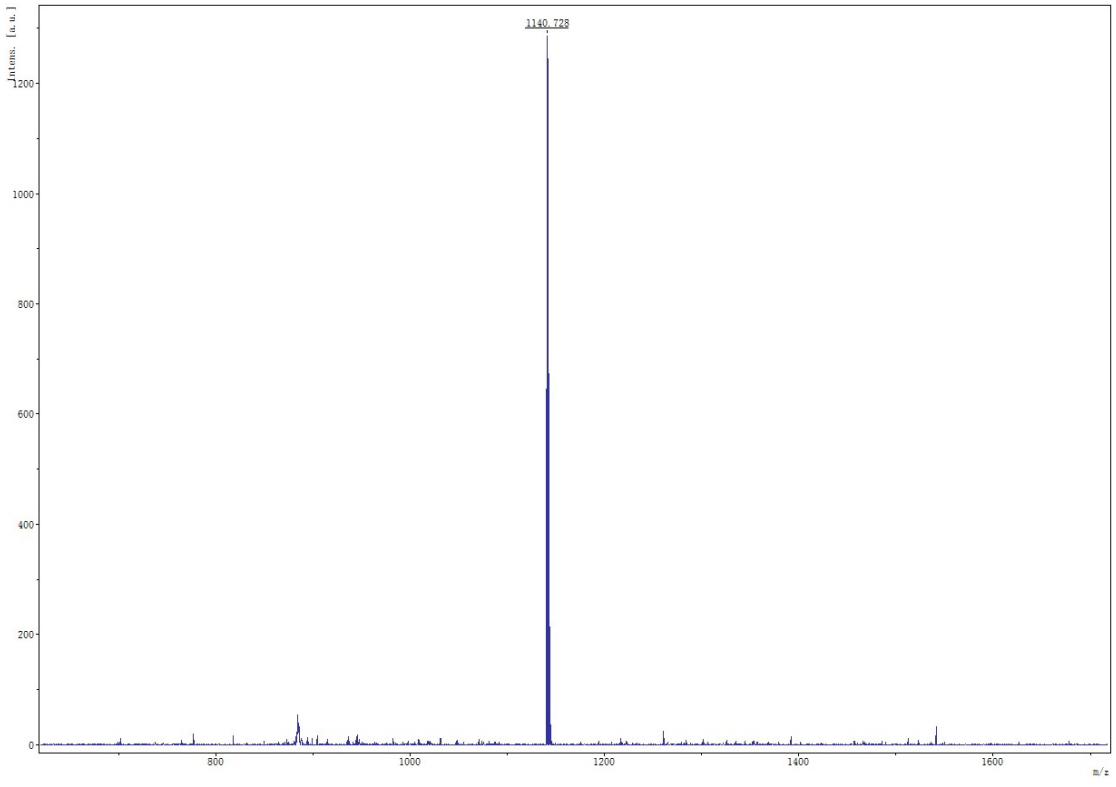

Figure S27. MS-MALDI spectrum of **FBT-DiTPA**.

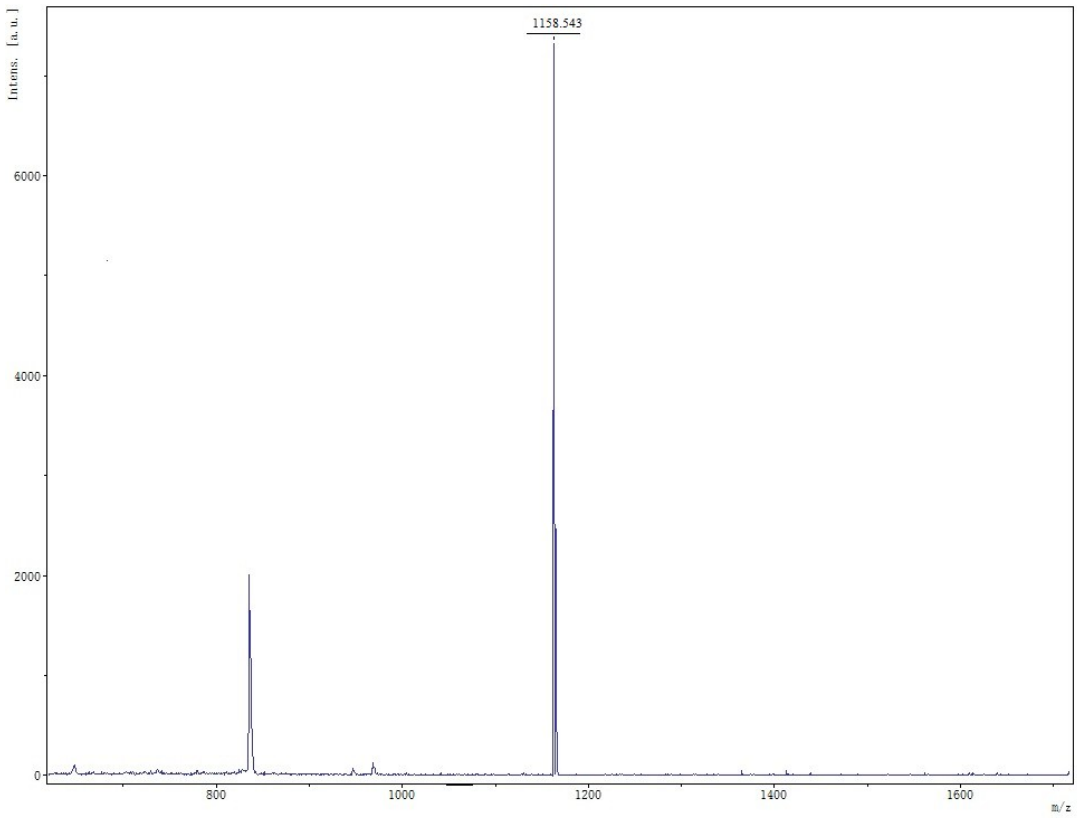

Figure S28. MS-MALDI spectrum of **FFBT-DiTPA**.

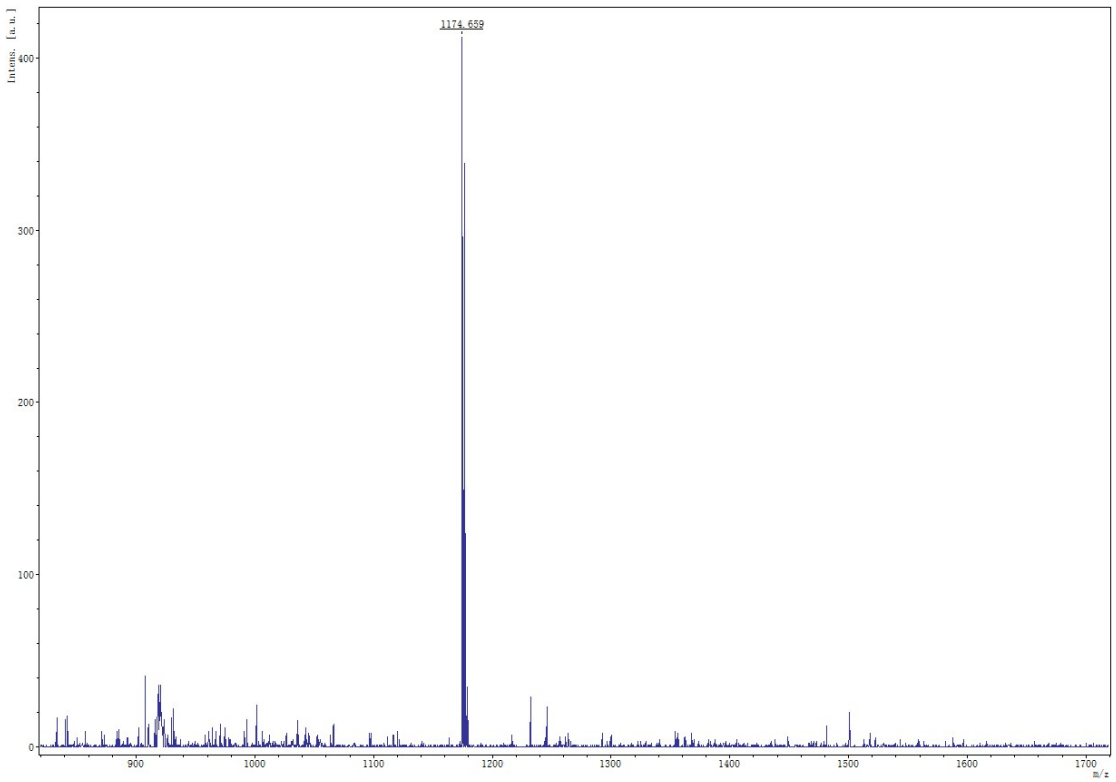

Figure S29. MS-MALDI spectrum of **FClBT-DiTPA**.

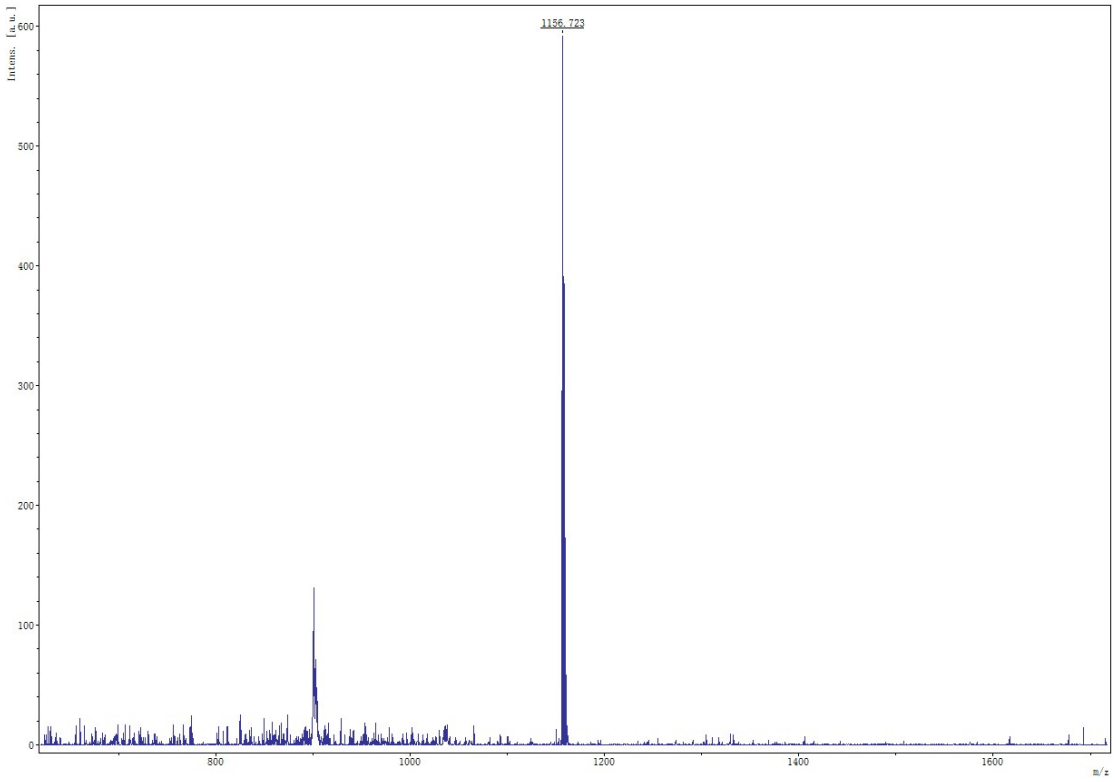

Figure S30. MS-MALDI spectrum of **ClBT-DiTPA**.

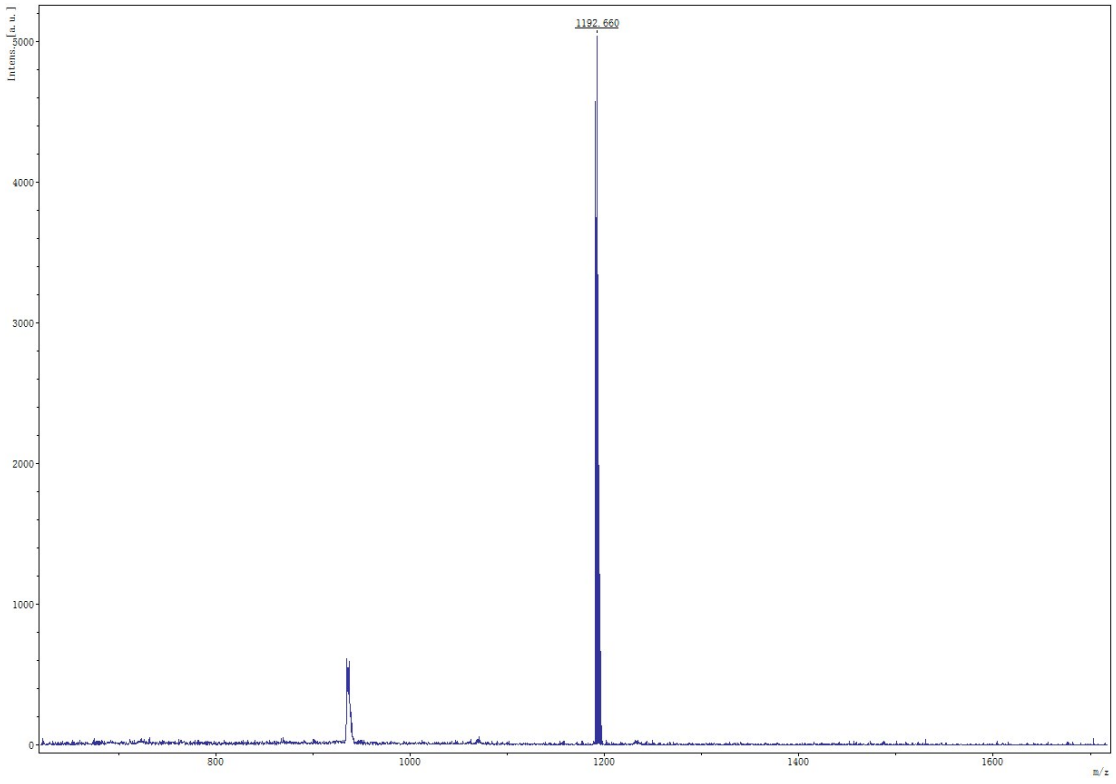

Figure S31. MS-MALDI spectrum of **ClClBT-DiTPA**.

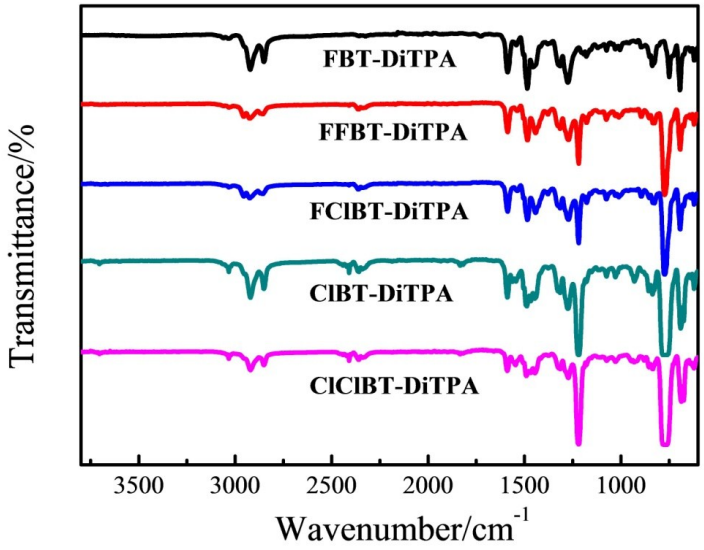

Figure S32. FT-IR spectra of **FBT-DiTPA**, **FFBT-DiTPA**, **FClBT-DiTPA**, **ClBT-DiTPA**, and **ClClBT-DiTPA.**